AD-A169 656 INDUCED INSULATOR VOLTAGE IN TRANSMITTER ANTENNA GUY CABLES(U) NAVAL OCEAN SYSTEMS CENTER SAN DIEGO CA P M HANSEN ET AL. DEC 85 NOSC/TD-868 1/1

UNCLASSIFIED F/G 9/3 NL

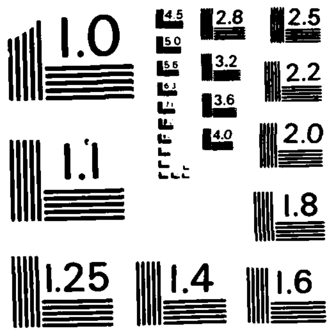

MICROCOPY RESOLUTION TEST CHART

NATIONAL BUREAU OF STANDARDS - 1963 - A

(12)

TD 868

TD 868

Technical Document 868
December 1985

INDUCED INSULATOR VOLTAGE IN TRANSMITTER ANTENNA GUY CABLES

P. M. Hansen
D. G. Fern
C. F. Ramstedt

Naval Ocean Systems Center
San Diego, California 92152

NAVAL OCEAN SYSTEMS CENTER

San Diego, California 92152-5000

F. M. PESTORIUS, CAPT, USN
Commander

R. M. HILLYER
Technical Director

ADMINISTRATIVE INFORMATION

This task was conducted by personnel in the Systems Engineering and Analysis Branch, Code 831, and Radiation Physics Branch, Code 524, during the period from July to December, 1985, with OM&N funding under the sponsorship of Space and Naval Warfare Systems Command, PDW-110-1415.

Released by
J.E. Richter, Head
Systems Engineering and
Analysis Branch

Under the authority of
E.R. Jahn, Head
Submarine and Strategic Systems
Division

UNCLASSIFIED
SECURITY CLASSIFICATION OF THIS PAGE

AD-A169656

REPORT DOCUMENTATION PAGE

1a REPORT SECURITY CLASSIFICATION UNCLASSIFIED	1b RESTRICTIVE MARKINGS
2a SECURITY CLASSIFICATION AUTHORITY	3 DISTRIBUTION/AVAILABILITY OF REPORT Approved for public release; distribution is unlimited.
2b DECLASSIFICATION/DOWNGRADING SCHEDULE	
4 PERFORMING ORGANIZATION REPORT NUMBER(S) NOSC TD 868	5 MONITORING ORGANIZATION REPORT NUMBER(S)
6a NAME OF PERFORMING ORGANIZATION Naval Ocean Systems Center; 6b OFFICE SYMBOL (if applicable)	7a NAME OF MONITORING ORGANIZATION
6c ADDRESS (City, State and ZIP Code) San Diego, CA 92152-5000	7b ADDRESS (City, State and ZIP Code)
8a NAME OF FUNDING/SPONSORING ORGANIZATION Space and Naval Warfare Systems Command; 8b OFFICE SYMBOL (if applicable) PDW-110	9 PROCUREMENT INSTRUMENT IDENTIFICATION NUMBER
8c ADDRESS (City, State and ZIP Code) Washington, DC 20363-5100	10 SOURCE OF FUNDING NUMBERS

PROGRAM ELEMENT NO	PROJECT NO	TASK NO	Agency Accession No.
OMN	S&NW	832-CM19	DN587 543

11 TITLE (include Security Classification)

Induced Insulator Voltage in Transmitter Antenna Guy Cables

12 PERSONAL AUTHOR(S)

P.M. Hansen, D.G. Fern, C.F. Ramstedt

13a TYPE OF REPORT	13b TIME COVERED	14 DATE OF REPORT (Year, Month, Day)	15 PAGE COUNT
Final	FROM Jul 1985 TO Dec 1985	December 1985	39

16 SUPPLEMENTARY NOTATION

17 COSATI CODES			18 SUBJECT TERMS (Continue on reverse if necessary and identify by block number)
FIELD	GROUP	SUB GROUP	

19 ABSTRACT (Continue on reverse if necessary and identify by block number)

A method is examined for the analytical determination, with very good accuracy, of the rf voltage that will be developed across insulators in transmitter guy cables. The Numerical Electromagnetics Code was used to develop the predictions, which were then compared with measurements conducted on a model antenna. Calculated and measured values of the mutual impedence (the ratio of induced voltage to antenna feedpoint current) were obtained for a scaled configuration containing a vertical radiator and one top-loading guy cable. Eighteen test conditions were examined, with nine insulator location patterns (i.e., one to five insulators) and two insulator capacitances. For those test conditions chosen to represent realistic antennas, the mean and maximum differences between calculated and measured mutual impedance values are 0.12 and 9.93 percent, respectively. This small difference indicates that the method is well suited both to engineering design considerations and to the investigation of the adequacy of insulator withstand-voltages at existing transmitter sites.

20 DISTRIBUTION/AVAILABILITY OF ABSTRACT [X] UNCLASSIFIED/UNLIMITED [ ] SAME AS RPT [ ] DTIC USERS	21 ABSTRACT SECURITY CLASSIFICATION UNCLASSIFIED

22a NAME OF RESPONSIBLE INDIVIDUAL	22b TELEPHONE (include Area Code)	22c OFFICE SYMBOL
P.M. Hansen	(619) 225-7302	Code 831

DD FORM 1473, 84 JAN

83 APR EDITION MAY BE USED UNTIL EXHAUSTED
ALL OTHER EDITIONS ARE OBSOLETE

UNCLASSIFIED
SECURITY CLASSIFICATION OF THIS PAGE

DD FORM 1473, 84 JAN

SUMMARY

OBJECTIVE

This task examined a method for the analytical determination, with very good accuracy, of the radio frequency (rf) voltage that will be developed across insulators in transmitter antenna guy cables. The Numerical Electromagnetics Code (NEC) was used to develop the predictions, which were then compared with measurements conducted on a model antenna.

RESULTS

Calculated and measured values of the mutual impedance, Z_{21}, which here is the ratio of induced voltage to antenna feed point current, were obtained for a scaled configuration containing a vertical radiator and one top-loading guy cable. Eighteen test conditions were examined, with nine insulator location patterns (i.e., one to five insulators) and two insulator capacitances. For those test conditions chosen to represent realistic antennas, the mean and maximum differences between calculated and measured values of Z_{21} are 0.12 and 9.93 percent, respectively.

This small difference between calculated and measured values indicates that the method is well suited both to engineering design applications and to the investigation of the adequacy of insulator withstand-voltages at existing transmitter sites.

CONTENTS

BACKGROUND

The rf voltage developed across each insulator in a transmitter antenna guy cable will be the result of capacitive and inductive coupling between the radiator and the guy cable and of the direct connection of the insulator-bearing cable across the antenna. The specification and selection of insulators has, in practice, been based on empirical methods, with the result that insulators may be installed which have either insufficient or unnecessarily high breakdown voltage ratings. The former condition will be discovered after a completed site has been put into operation. The extent to which the latter condition is present may never be revealed since there will be no overt performance effects.

However, a considerable price may have been paid for a more than adequate design. The difference between a sufficient design and one that is overly conservative may be measured in terms of hundreds to thousands of pounds of excess insulator weight. That excess will be cascaded in the weight of the tower, the guy cables and anchors, and the base insulator.

There is a need for a prediction procedure that yields insulator voltages to within generally accepted engineering design tolerances. Such a method will have application during the design of new transmitter sites as well as in the determination of antenna power limitations at existing sites.

INTRODUCTION

The NEC computer program can, in principle, be used to calculate voltages induced on guy cable insulators near a radiating element. To test and evaluate such an application, an antenna model was specified that would be both easily examined with NEC and assembled in the field for measurements.

The model was composed of a 6-meter vertical radiator with a feedpoint at the base (Figure 1). A single guy cable connected the top of the radiator to the ground screen. The combination formed a right triangle. The guy cable contained 14 small fixtures designed to hold capacitors to simulate insulators at various locations. Nine insulator-location configurations were examined, with between one and five capacitors in a given configuration (Figure 2). Shunts were installed in unused fixtures. A fixture with a capacitor installed is shown in the upper portion of Figure 3.

Each configuration was filled with 50-pF capacitors in one set of measurements and with 10-pF units in another. The former capacitance is in the range of values found at transmitter sites. The latter was included to facilitate observations of any effects on test results attributable to leakage and shunt capacitances associated with the test instrumentation.

The quantity required as a product of both analysis and measurement for each configuration is the ratio of voltage on a capacitor to the current into the antenna feedpoint, i.e., Z_{21}. A direct measurement of capacitor voltage was not practical because placing a voltmeter, an operator, and a step ladder near the guy cable would alter the voltage-inducing fields. A technique based on reciprocity was devised which allowed the placement of the voltmeter on the ground screen adjacent to the feedpoint while a small battery-powered rf signal source was connected across and suspended from the insulator (fixture) under examination (Figure 3). The voltmeter's input capacitance still had a significant influence, and the voltages measured were adjusted to remove the effect of that influence.

The effectiveness of the NEC in this application is evaluated through an examination of the differences between calculated and measured values of Z_{21} obtained for each test condition. Calculations and measurements of the antenna input (feedpoint) impedance, Z_A, are included in this work.

The following paragraphs provide a brief introduction to the NEC, a description of the test configurations, the theoretical basis for the measurement process, and an evaluation of the method. All results of the analyses and measurements are presented in Appendices A and B.

NUMERICAL ELECTROMAGNETICS CODE

NEC is an advanced computer code designed for the analysis and description of fields radiated from current-carrying structures and of currents and voltages induced by incident fields. The NEC program is based on numerical solutions of both electric-field and magnetic-field integral equations to determine the electromagnetic response of general structures. The electric-field integral equation is well suited to the modeling of thin-wire structures of small or vanishing conductor volume, while the magnetic-field integral equation is applicable to very large structures, especially those with extensive smooth surfaces. The electric-field integral equation in NEC has been specifically adapted for applications with thin wires.* The wires may be in free space or over a perfect or lossy ground.

An NEC model may include nonradiating networks and transmission lines, perfect and imperfect conductors, lumped-element loading, and both perfect and imperfect ground planes. Excitation may be via an applied voltage, an incident plane wave, or a constant-current source. Program outputs include induced currents and charges, near- and far-zone electric and magnetic fields, and impedances and admittances. Other commonly used parameters available include gain and directivity, power, and antenna-to-antenna coupling.

NEC was developed at the Lawrence Livermore National Laboratory under joint sponsorship of the Naval Ocean Systems Center and the Air Force Weapons Laboratory, with additional sponsorship by the U.S. Army Communications-Engineering Installation Agency, Fort Huachuca. The NEC user community includes 17 government organizations and over 39 domestic and foreign companies and universities.

ANTENNA–GUY CABLE TEST CONFIGURATIONS

The nine insulator test configurations examined (Figure 2), were designed to represent patterns present at operating sites, to constitute a reasonable evaluation of NEC predictions of insulator voltages, and to investigate the position dependency of voltage where multiple insulators are present.

*G.J. Burke and A.J. Pogio, Numerical Electromagnetics Code (NEC) – Method of Moments, NOSC TD 116, Vol. 1, January, 1981.

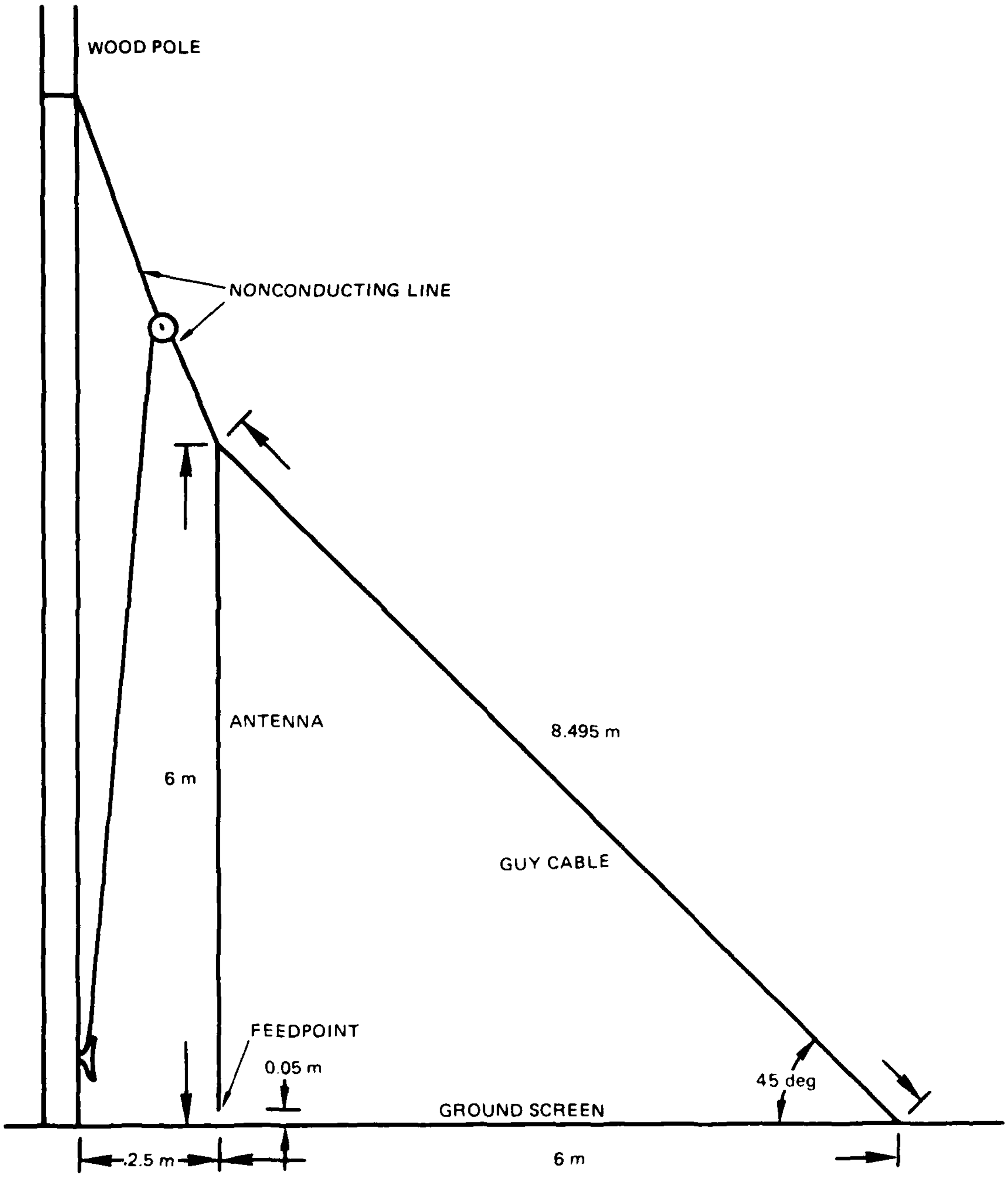

Figure 1. Field test implementation.

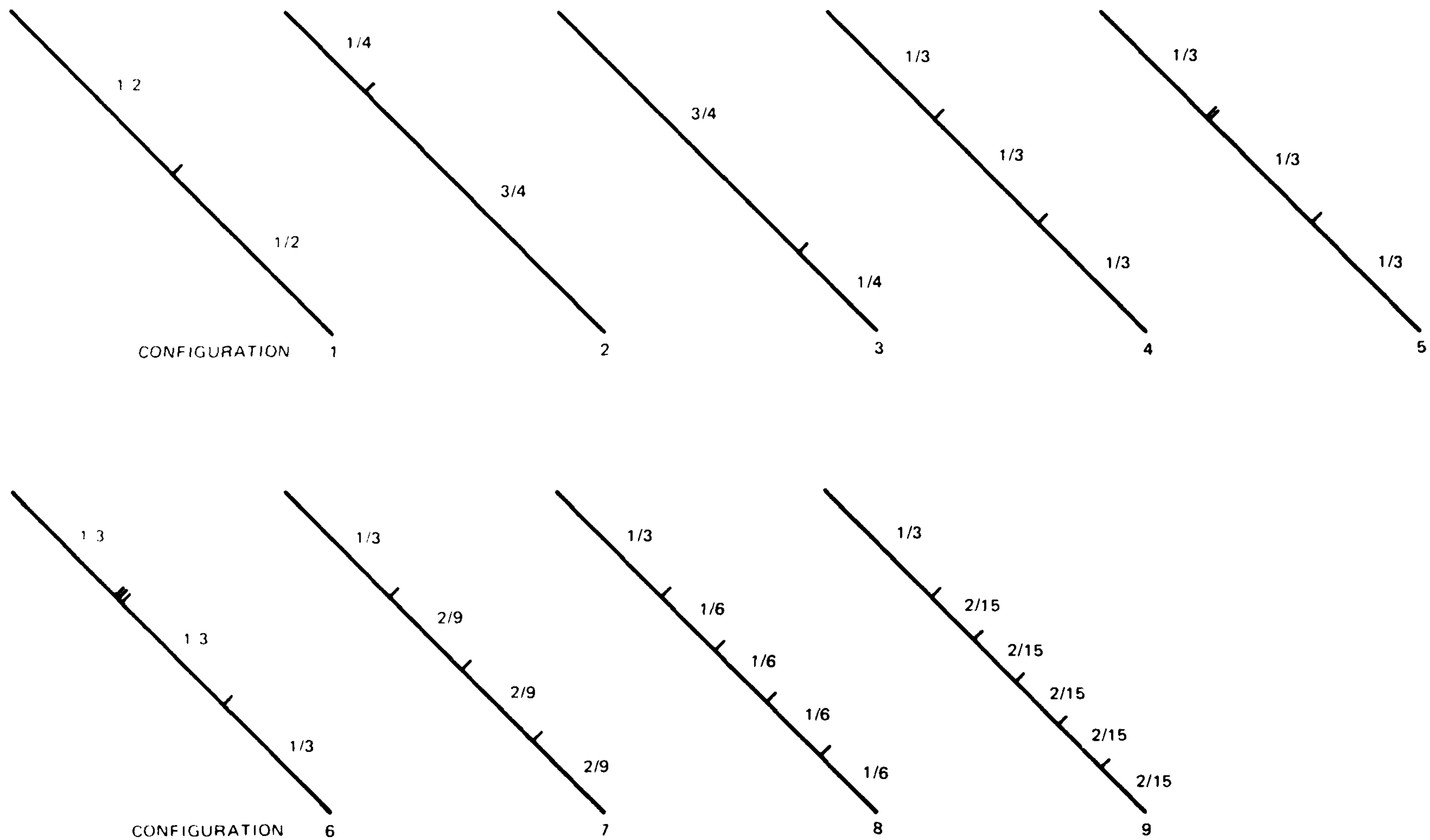

Figure 2. Insulator test configurations with fixture separations shown as fractions of the total guy cable length. The uppermost capacitor holding fixtures in configurations 5 and 6 are immediately adjacent to each other, and the installed capacitors are separated by 5.3 cm center to center.

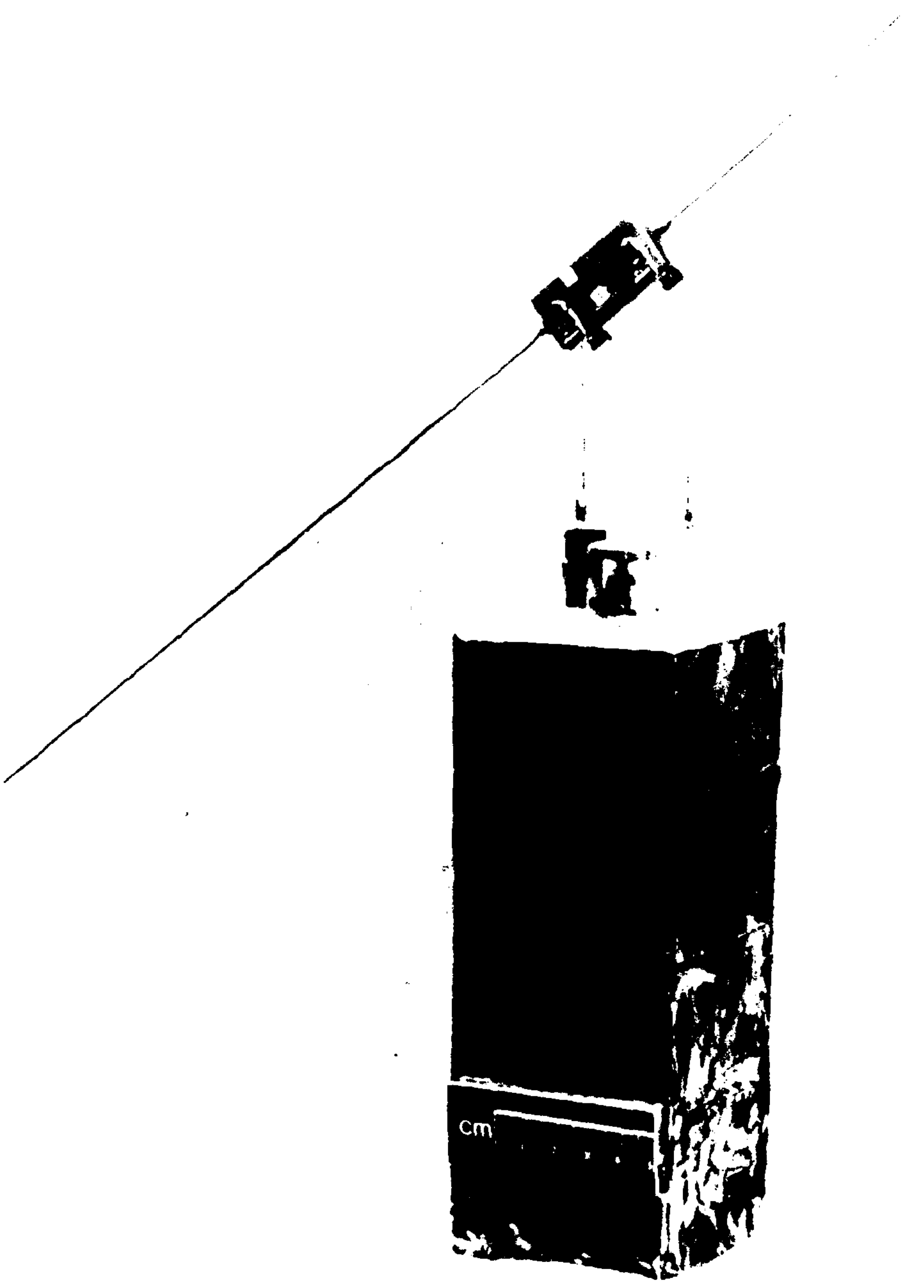

Figure 3. Capacitor holding fixture with the signal source and a capacitor attached.

A change from one configuration to another and between capacitor sets was accomplished by lowering the wire with the insulated line shown in Figure 1. The size of the antenna – guy cable combination was chosen to provide convenience in handling and a loop length very small relative to a wavelength at the test frequency of 2.0 MHz. The test frequency was placed in a region of the spectrum where measurements indicated a broad noise minimum.

Capacitors manufactured for good temperature stability and high-frequency operation were used in the tests and individually measured at the test frequency. Capacitances of the two sets ranged from 48.6 to 48.9 pF for the 50-pF set and from 10.1 to 10.2 pF for the 10-pF set. The average of the capacitances of the individual capacitor holding fixtures was 1.5 pF. Actual capacitances should be within ±0.3 pF of the indicated values. Capacitances used in each test configuration are given with the measurement data in Appendix A.

MEASUREMENT PROCESS

PROCESS BASIS

The objective is the measurement across a capacitor of a voltage induced by a current flowing in the antenna feedpoint and the calculation of the quantity Z_{21}. As noted above, a voltage measurement at a capacitor's location would inject indeterminable errors in the data. That difficulty can be circumvented by reversing the locations of the signal source and voltmeter. From reciprocity it is known that Z_{21} in one direction through a passive circuit will equal Z_{21} in the opposite direction.

It remains necessary to determine the current from the signal source while it is attached to a guy cable that is in the elevated position. This will be accomplished by a procedure which permits a determination, at the feedpoint, of the load on the signal source when it is on an elevated cable. When the value of that load and the signal source voltage are known, the current can be calculated. The procedure is described in the following paragraphs.

The circuit shown in Figure 4 represents the circuit under measurement when the guy cable is elevated.

For the two relay contact conditions, (1) and (2) apply:

$$e_t = (i_t - \text{low})\,(R_S - jX_{C_t}) \qquad \text{relay open} \tag{1}$$

$$e_t = (i_t - \text{high})\,(-jX_{C_t}) \qquad \text{relay closed,} \tag{2}$$

where i_t - low is the current with R_S in the circuit, and i_t – high is the current with R_S not in the circuit.

Combining (1) and (2) and solving for X_{C_t} results in

$$X_{C_t} = \left(\frac{(i_t - \text{low})^2}{(i_t - \text{high})^2 - (i_t - \text{low})^2}\right)^{1/2} \cdot \tag{3}$$

From the definition of Z_{21} in (4), two expressions are obtained as given in (5) and (6):

$$Z_{21} = \frac{e_o}{i_i} \tag{4}$$

$$i_i - \text{low} = \frac{e_o - \text{low}}{Z_{21}} \tag{5}$$

$$i_i - \text{high} = \frac{e_o - \text{high}}{Z_{21}} \quad , \tag{6}$$

where e_o – low is the feedpoint signal voltage with R_S in the circuit, and e_o – high is the feedpoint signal voltage with R_S not in the circuit.

Substituting (5) and (6) into (3) results in

$$X_{C_t} = R_S \left(\frac{(e_o - \text{low})^2}{(e_o - \text{high})^2 - (e_o - \text{low})^2} \right)^{1/2} \quad . \tag{7}$$

Values of R_S were selected to insure an adequate difference between the high and low output signal levels. If they are very close in magnitude, the accuracy of the calculated X_{C_t} can be degraded. Three values of R_S were used: 1, 5.1, and 10 kilohms.

The input voltage, e_i, was measured before and after each antenna-guy cable test configuration was put in the raised position, an interval of 2 to 3 minutes. If any drift was observed in the magnitude of e_i, then the average of the two values was used in the calculation of i_i. Drift, when observed, was typically less than 0.3 percent.

INSTRUMENTATION

The signal source was designed specifically for this application. The circuit contained a crystal-controlled oscillator, a bandpass filter, and a low-output-impedance amplifier. The relay was under the control of an independent time-driver. Three 9-V batteries provided power for about 3 hours of continuous operation.

All voltage measurements were made with an HP model 3586B Selective Level Meter combined with an HP model 1124A Active Probe. A bandpass of 3200 Hz was used, which was automatically centered at the test frequency. The probe's input resistance is 10 megohoms, shunted by a capacitance adjusted to near 10 pF during manufacture. The resistive component was large enough to not affect measurements of e_o; however, the capacitive component did. As a result, procedures for probe loading corrections were developed and are discussed in the next section.

CORRECTIONS FOR PROBE LOADING

For the test configurations in this work, the probe capacitance will be large enough to affect the voltage measurements used to determine Z_{21} and Z_A. This is not likely to be a problem at operating sites because of the large capacitance of base insulators. The bases for the measurement corrections used in this work will be developed from the circuit in Figure 5.

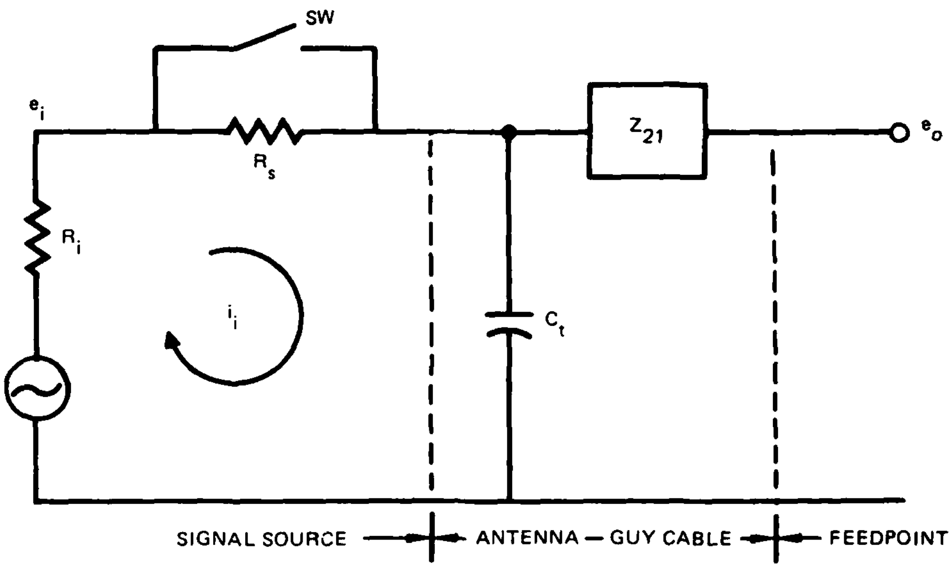

Figure 4. Measurement equivalent circuit. Circuit elements are defined as follows:

R_i = source internal resistance, 6 ohms.

e_i = signal source voltage.

R_s = current-limiting resistance, in the range of 1 to 10 kilohms.

SW = relay, shunts R_s for 5 seconds at 10-second intervals.

i_i = signal source current.

C_t = total capacitance as seen by the signal source.

Z_{21} = mutual impedance, to be calculated.

e_o = signal voltage at the feedpoint.

The total reactance across the feedpoint terminals with the probe attached is given by

$$X_T = \frac{X_P X_A}{X_P + X_A} \quad , \tag{8}$$

where X_P is the reactance of the probe capacitance, and X_A is the reactance of the feedpoint capacitance.

Solving (8) for X_A results in

$$X_A = \frac{X_P X_T}{X_P - X_T} \quad . \tag{9}$$

Both X_P and X_T were directly measured, the latter for each test configuration in which the guy cable was in the elevated position. The measurement of reactance will be described with reference to Figure 6.

The relationships in (10) and (11) follow directly from Figure 6:

$$e_i = i_i (R_S - jX_C) \tag{10}$$

$$e_o = i_i X_C . \tag{11}$$

Combining (10) and (11) and solving for X_C leads to

$$X_C = \frac{R_S}{\left((e_i/e_o)^2 - 1\right)^{1/2}} \quad . \tag{12}$$

When only the probe is on the signal source, the resulting X_C is that of the probe capacitance. When that combination is connected to the feedpoint, the X_C becomes the X_T required in (9). Thus the solution of (9) provides a feedpoint reactance free of probe loading.

In practice, all measurements made relative to X_P and X_T were conducted with a consistent instrumentation geometry and procedural routine. Also, the reactance obtained for a given capacitor was slightly dependent upon the value of R_S used, probably because of a small shunting capacitance within the signal source. Therefore, the values of X_P and X_A used in a given solution of (9) were obtained with the same R_S.

Corrections for the effects of probe loading were required in one other part of the data reduction process. During measurements of e_o for the Z_{21} calculations, the voltages recorded were low because of probe loading. Determining the extent to which an e_o is lowered will permit calculation of a correct Z_{21}.

Equations (13) and (14) can be written directly from an inspection of Figure 5.

$$e_o\text{-meas} = e_{oc} \frac{X_P}{X_P + X_A} \qquad \text{probe connected} \tag{13}$$

$$e_{oc} = e_o \qquad \text{probe not connected} \tag{14}$$

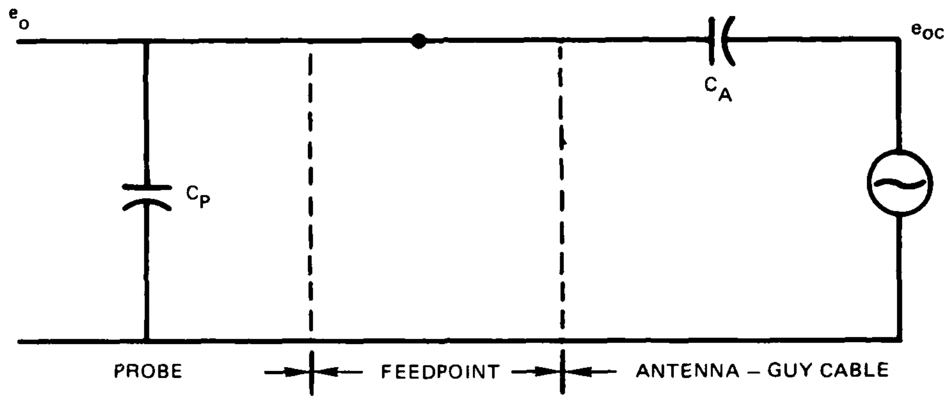

Figure 5. Feedpoint with probe connected. C_p is probe capacitance, C_A is feedpoint capacitance, and e_{oc} is open-circuit voltage.

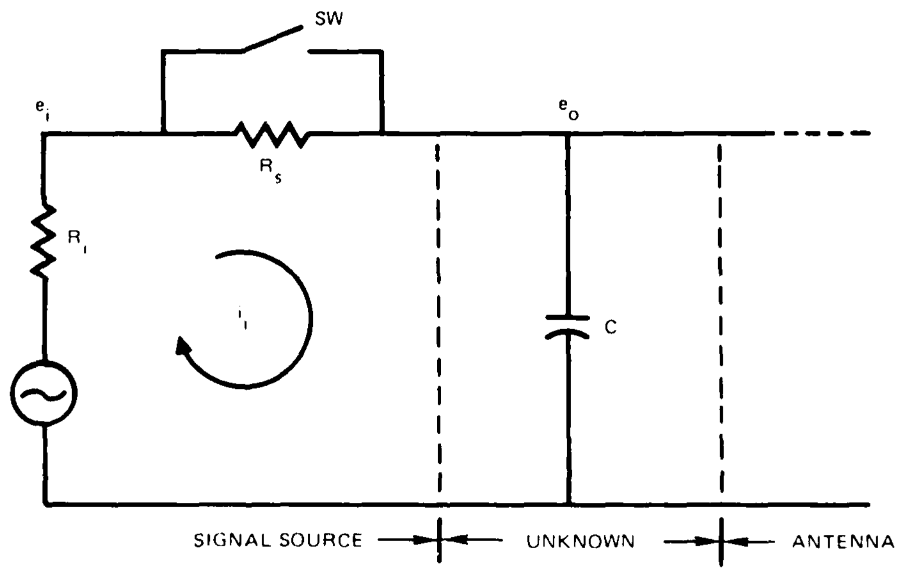

Figure 6. Reactance measurement circuit. C is any capacitance under examination.

Solving for the ratio of the two voltage terms results in

$$\frac{e_{oc}}{e_o - \text{meas}} = \frac{X_A + X_P}{X_p} \quad . \tag{15}$$

The solution of (15) was used as a correction factor, multiplied by an apparent Z_{21} to obtain its correct value.

RESULTS

The results are very good both in terms of comparisons between calculated and measured parameter values and in terms of the correspondence between these data and existing knowledge about insulator voltage induction at operating transmitter sites. All calculated and measured values of Z_{21}, the voltage induced by a given input current, and Z_A, the antenna feedpoint input impedance, are presented in Appendix A for each configuration and in a format that allows easy comparisons. Tabulations of NEC computations alone are given in Appendix B. Several general observations are discussed in the following paragraphs.

Table 1 presents a statistical summary of all data. For Z_A all measured values were less than those calculated by a very small amount. In the discussion of the Z_{21} results there are several suggestions relative to conditions that could have been responsible for the differences between calculated and measured values. Those suggestions also apply in general to the Z_A results.

Table 1. Percent differences of measured parameters from calculated parameters to all configurations

	50-pF Set		10-pF Set	
	Z_{21}	Z_A	Z_{21}	Z_A
Mean	0.12	−2.83	−4.69	−3.86
SD	4.33	1.42	8.81	2.01
Extrema	+9.93	−0.75	+21.39	−1.62
	−8.20	−5.09	−15.09	−7.46

For Z_{21} in the 50-pF data set, the mean (Table 1) is strikingly small, while the SD (standard deviation) and extrema indicate that there is some spread in the differences. The basis for that spread is somewhat systematic. The differences tend to be small or positive in sign for insulator locations high on the guy cable, and larger and negative in sign for those low on the cable. This is most clearly seen in Figures A-15 and A-17. Although less conspicuous, this same pattern is present in the 10-pF data set.

That pattern of differences, increasing negatively downward on the guy cable, could have two causes not accounted for in this initial NEC trial. One is associated with the physical length, or height, of the signal source. The fraction of the distance between the guy cable and the ground screen occupied by the signal source will increase as the signal source is moved lower along the cable. Therefore, the leakage capacitance between insulator locations and ground will be systematically altered by the measurement process.

The second is associated with the NEC use requirement that all wire dimensions must be carefully specified. The capacitor holding fixtures represent short sections of increased wire size that were not differentiated from the 16-AWG connecting conductor sections. The density of holding fixtures increased toward the lower end of the guy cable, and the resulting increase in the average wire diameter could have introduced a systematic effect on capacitive and inductive coupling.

Both of these potential causes for a systematic pattern in the differences between calculated and measured values can be examined through successive NEC trials in that both can easily be specified in the input parameters. A third potential cause was eliminated in the test design. The weight of the signal source can pull down on the guy cable to form two segments with different angles above the ground plane. The lower segment, with the decreased angle, would always have an increased leakage capacitance. A 20-foot-long pole of 1- by 2-inch kiln-dried white pine was used to support the guy cable near the signal source attachment point so that the guy cable was always straight at the time of a measurement. Several tests were conducted to establish that neither the pole nor the person holding it had an observable influence on a measurement.

During the design of this investigation, 50-pF capacitors were selected to simulate insulators because that value was conveniently within the range of insulator capacitances found in a brief survey of antenna sites. The 10-pF set was added in order to gain knowledge on the practical consequences of treating systems with very small capacitive elements.

If the 50-pF data set is used as a basis for judgement, the 10-pF data set can be described as having both large differences between calculated and measured values and greater variability in those differences. Any of several circumstances could have contributed to that result. The limits of uncertainty or error in capacitor measurements were estimated to be ±0.3 pF, which for the smaller capacitor set is a much larger percentage. The capacitances of the capacitors used in the measurements, given on each figure in Appendix A, deviated from those used in the NEC calculations by amounts which, as percentages, were large in the 10-pF set. Any leakage capacitance in shunt with the R_S resistor in the signal source will introduce the larger error in the 10-pF test set data. (The signal source was reconstructed once to reduce that leakage capacitance from about 2 pF to some much smaller value.) If the circumstances noted above relative to wire size specification and signal source body length could have had an effect in the 50-pF data set, then that effect should be larger in the 10-pF data set.

In the above paragraphs, the results of this investigation were examined in terms of difference between calculated and measured values. Traditional guy cable design practice offers another basis. It is well established that the voltage induced across an insulator increases as the insulator is placed higher on the cable, closer to the antenna tower. Where insulators are required very near the upper end of the cable, they are frequently placed there in closely spaced groups in order to reduce the potential across each to a level below breakdown. Both the calculated and measured values of Z_{21} show the same pattern: the higher the location examined along the cable, the higher the value of Z_{21}.

CONCLUSIONS

The results indicate that with the NEC, the rf voltages induced on one or more insulators in guy cable can be calculated to within a range of uncertainty that is quite acceptable for design. This conclusion is based on a comparison between the values of Z_{21} measured on a scaled vertical antenna with a single guy cable and those derived analytically for the same model.

Nine configurations of insulator locations, one to five per configuration, were examined, with each filled in turn by 50-pF and 10-pF capacitors. For the 50-pF data set, all measured values of Z_{21} were within 10 percent of calculated values. For the 10-pF data set, the maximum difference was just over 21 percent. All results are presented in Appendices A and B and summarized in Table 1.

Another basis for the evaluation of the results of this investigation can be found in the correspondence between both the calculated and measured values of Z_{21} on the one hand and, on the other, the traditional practice of locating insulator on operating antennas. Both indicate that the induced voltage increases as an insulator is located higher on a guy cable, closer to the antenna. Frequently, insulators near the top of a cable are placed there in closely spaced groups so as to reduce the voltage across each to a level below breakdown.

The 50-pF capacitor set was selected because it represented reasonably well an average of the insulator capacitances found in a brief survey of operating antennas. The 10-pF set was added in order to gain experience in the treatment of systems containing low-capacitance elements. With the latter set, in contrast to the former, the measurements did show greater variability and larger differences between calculated and measured values. Several possible reasons for that contrast between data sets were discussed in the previous section.

There was a systematic variation in the differences between calculated and measured values of Z_{21}. Differences were small or positive in sign (i.e., measured is larger than calculated) for the higher insulator locations and larger and negative for those lower on the guy cable. Two physical characteristics of the test model implementation not included in the NEC input data might have been responsible. The body of the signal source could add shunt capacitance between the insulator location under examination and ground, with the magnitude increasing as it is moved toward the lower end of the cable. Also, the capacitor holding fixtures effectively create short sections of increased wire diameter in the guy cable, and the average interval between fixtures decreased toward the lower end of the cable. It would be useful for tutorial reasons to run additional NEC trials to identify and characterize the specific causes of the systematic variations.

For practical reasons it would be very useful to further evaluate this class of NEC application with an examination of an antenna that has a full set of guy cables. A full-scale operating site should be considered for the task, and, if possible, a site which has had occurrences of insulator corona and breakdown. Additional benefits of such an investigation would include an evaluation of traditional insulator specification practices and of limitations on an antenna's operating power.

The conduct of follow-on verification tests could be simpler with a full-scale antenna because, depending on the site selected, many or all of the problems associated with shunt and leakage capacitances found in this work with a model will not be present. A somewhat larger signal source would be required, and a site rigger would have to be employed to carry the instrument to a number of insulators.

Differences between measured and NEC-produced results will probably be larger for full-scale antennas, in contract to models, because stray capacitances not accounted for in this work can be more than proportionally larger at an operating station. Therefore, with the existing data set as a basis, the introduction of stray capacitances in the NEC input parameters should be practiced to obtain the best correspondence between measurements and calculations.

APPENDIX A

MEASURED AND CALCULATED VALUES OF Z_{21} AND Z_A FOR ALL TEST SITUATIONS

FEEDPOINT

NEC	
Z_A	ϕ
561.8	-89.98

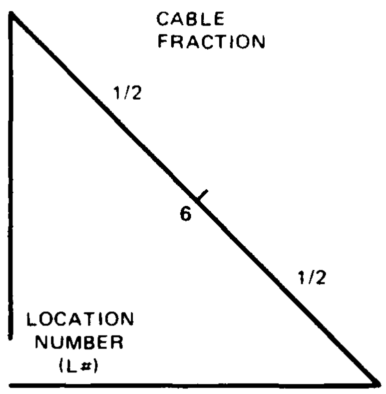

GUY CABLE

	CAPACITANCE		NEC	
L#	ACTUAL	NEC	Z_{21}	ϕ
6	50.1	50.0	763.6	90.02

MEASURED

$R_S = 1K$

Z_A	D
557.6	-0.75

MEASURED

$R_S = 1K$

L#	Z_{21}	D
6	770.3	0.88

UNITS: Z_A, OHMS
Z_{21}, OHMS
ϕ, DEGREES
D, PERCENT DIFFERENCE RE NEC
R_S, OHMS
CAPACITANCE, PICOFARADS, WITH FIXTURE

Figure A-1. Configuration 1, 50-pF set, Z_{21} and Z_A data.

FEEDPOINT

NEC

Z_A	ϕ
986.7	-89.96

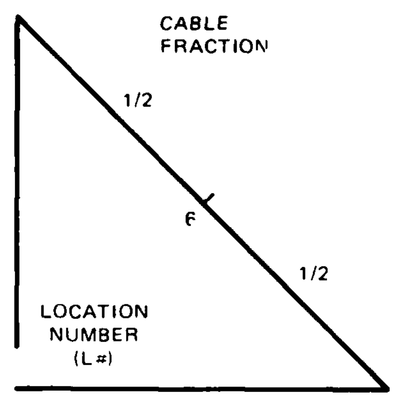

MEASURED

$R_S = 1K$

Z_A	D
956.4	-3.07

GUY CABLE

	CAPACITANCE		NEC	
L#	ACTUAL	NEC	Z_{21}	ϕ
6	11.6	11.0	1128.4	90.04

MEASURED

$R_S = 1K$

L#	Z_{21}	D
6	1115.0	-1.19

UNITS: Z_A, OHMS
Z_{21}, OHMS
ϕ, DEGREES
D, PERCENT DIFFERENCE RE NEC
R_S, OHMS
CAPACITANCE, PICOFARADS, WITH FIXTURE

Figure A-2. Configuration 1, 10-pF set, Z_{21} and Z_A data.

FEEDPOINT

NEC	
Z_A	ϕ
641.8	-89.98

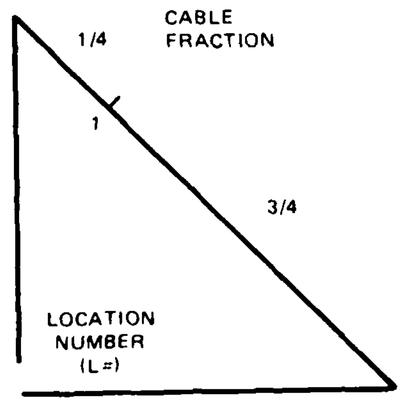

GUY CABLE

	CAPACITANCE		NEC	
L#	ACTUAL	NEC	Z_{21}	ϕ
1	50.4	50.0	857.4	90.01

MEASURED

$R_S = 1K$

Z_A	D
633.1	-1.36

MEASURED

$R_S = 1K$

L#	Z_{21}	D
1	853.8	-0.42

UNITS: Z_A, OHMS
Z_{21}, OHMS
ϕ, DEGREES
D, PERCENT DIFFERENCE RE NEC
R_S, OHMS
CAPACITANCE, PICOFARADS, WITH FIXTURE

Figure A-3. Configuration 2, 50-pF set, Z_{21} and Z_A data.

FEEDPOINT

NEC	
Z_A	ϕ
1193.3	-89.97

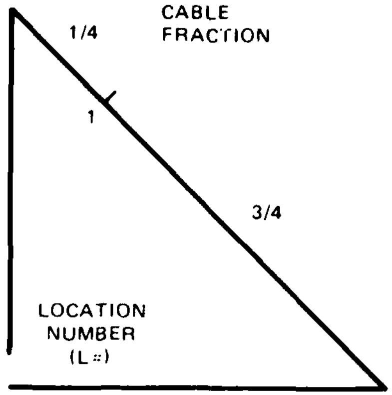

GUY CABLE

	CAPACITANCE		NEC	
L#	ACTUAL	NEC	Z_{21}	ϕ
1	11.6	11.0	1335.5	90.03

MEASURED

$R_S = 1K$

Z_A	D
1174.0	-1.62

MEASURED

$R_S = 1K$

L#	Z_{21}	D
1	1334.0	-0.11

UNITS: Z_A, OHMS
Z_{21}, OHMS
ϕ, DEGREES
D, PERCENT DIFFERENCE RE NEC
R_S, OHMS
CAPACITANCE, PICOFARADS, WITH FIXTURE

Figure A-4. Configuration 2, 10-pF set, Z_{21} and Z_A data.

FEEDPOINT

NEC	
Z_A	ϕ
481.7	-89.97

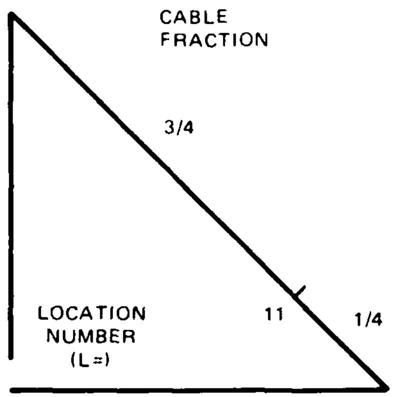

GUY CABLE

	CAPACITANCE		NEC	
L=	ACTUAL	NEC	Z_{21}	ϕ
11	50.1	50.0	703.3	90.02

MEASURED $R_S = 1K$

Z_A	D
467.6	-2.93

MEASURED $R_S = 1K$

L#	Z_{21}	D
11	674.5	-4.09

UNITS: Z_A, OHMS
Z_{21}, OHMS
ϕ, DEGREES
D, PERCENT DIFFERENCE RE NEC
R_S, OHMS
CAPACITANCE, PICOFARADS, WITH FIXTURE

Figure A-5. Configuration 3, 50-pF set, Z_{21} and Z_A data.

FEEDPOINT

NEC	
Z_A	ϕ
814.3	-89.96

MEASURED

$R_S = 1K$

Z_A	D
764.8	-7.00

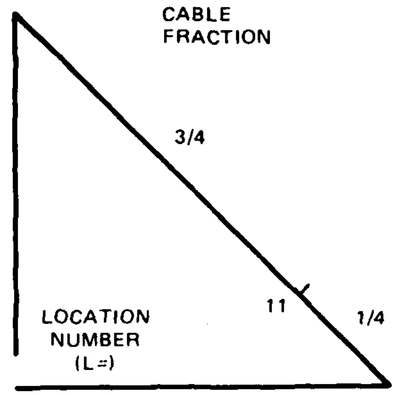

GUY CABLE

	CAPACITANCE		NEC	
L#	ACTUAL	NEC	Z_{21}	ϕ
11	11.7	11.0	990.4	90.03

MEASURED

$R_S = 1K$

L#	Z_{21}	D
11	936.4	-5.45

UNITS Z_A, OHMS
Z_{21}, OHMS
ϕ, DEGREES
D, PERCENT DIFFERENCE RE NEC
R_S, OHMS
CAPACITANCE, PICOFARADS, WITH FIXTURE

Figure A-6. Configuration 3, 10-pF set, Z_{21} and Z_A data.

FEEDPOINT

NEC	
Z_A	ϕ
869.6	-89.99

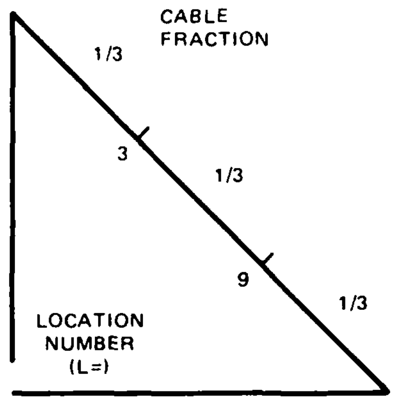

GUY CABLE

	CAPACITANCE		NEC	
L#	ACTUAL	NEC	Z_{21}	ϕ
3	50.1	50.0	579.2	90.02
9	50.4	50.0	447.8	90.03

MEASURED $R_S = 1K$

Z_A	D
830.7	-4.47

MEASURED $R_S = 1K$

L#	Z_{21}	D
3	576.9	-0.40
9	437.1	-2.39

UNITS: Z_A, OHMS
Z_{21}, OHMS
ϕ, DEGREES
D, PERCENT DIFFERENCE RE NEC
R_S, OHMS
CAPACITANCE, PICOFARADS, WITH FIXTURE

Figure A-7. Configuration 4, 50-pF set, Z_{21} and Z_A data.

FEEDPOINT

NEC	
Z_A	ϕ
1207.0	-89.96

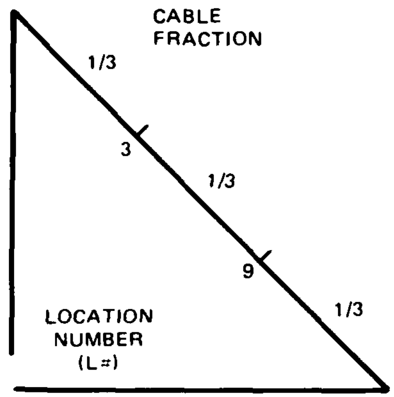

GUY CABLE

	CAPACITANCE		NEC	
L#	ACTUAL	NEC	Z_{21}	ϕ
3	11.7	11.0	907.3	90.02
9	11.6	11.0	408.1	90.07

MEASURED

R_S = 1K	
Z_A	D
1117.0	-7.46

MEASURED

	R_S = 1K		R_S = 10K	
L#	Z_{21}	D	Z_{21}	D
3	865.4	-4.62	905.4	-0.21
9	402.1	-1.47		

UNITS Z_A, OHMS
Z_{21}, OHMS
ϕ, DEGREES
D, PERCENT DIFFERENCE RE NEC
R_S, OHMS
CAPACITANCE, PICOFARADS, WITH FIXTURE

Figure A-8. Configuration 4, 10-pF set, Z_{21} and Z_A data.

FEEDPOINT

NEC	
Z_A	ϕ
1009.3	-89.96

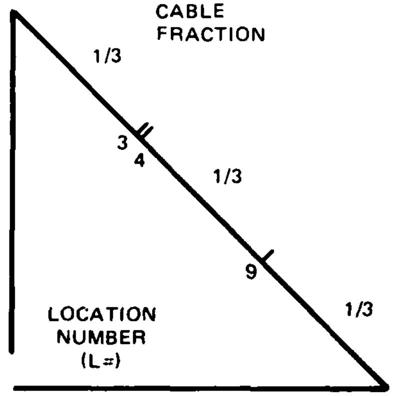

GUY CABLE

	CAPACITANCE		NEC	
L#	ACTUAL	NEC	Z_{21}	ϕ
3	50.1	50.0	411.5	90.02
4	50.1	50.0	407.5	90.03
9	50.1	50.0	328.1	90.05

MEASURED

R_S = 1K	
Z_A	D
971.7	-3.73

MEASURED

	R_S = 1K		R_S = 5.1K	
L#	Z_{21}	D	Z_{21}	D
3	423.0	2.79	432.9	5.20
4	400.2	-1.79	409.3	0.44
9			327.8	-0.09

UNITS: Z_A, OHMS
Z_{21}, OHMS
ϕ, DEGREES
D, PERCENT DIFFERENCE RE NEC
R_S, OHMS
CAPACITANCE, PICOFARADS, WITH FIXTURE

Figure A-9. Configuration 5, 50-pF set, Z_{21} and Z_A data.

FEEDPOINT

NEC	
Z_A	ϕ
1274.1	-89.96

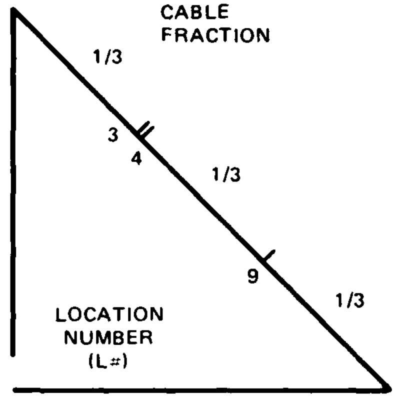

MEASURED

R_S = 5.1K

Z_A	D
1231.0	-3.38

GUY CABLE

	CAPACITANCE		NEC	
L#	ACTUAL	NEC	Z_{21}	ϕ
3	11.6	11.0	557.5	90.02
4	11.7	11.0	536.8	90.02
9	11.6	11.0	281.4	90.10

MEASURED

R_S = 5.1K

L#	Z_{21}	D
3	585.0	4.93
4	474.0	-11.70
9	263.6	-6.33

UNITS: Z_A, OHMS
Z_{21}, OHMS
ϕ, DEGREES
D, PERCENT DIFFERENCE RE NEC
R_S, OHMS
CAPACITANCE, PICOFARADS, WITH FIXTURE

Figure A-10. Configuration 5, 10-pF set, Z_{21} and Z_A data.

FEEDPOINT

NEC	
Z_A	ϕ
1098.9	-89.97

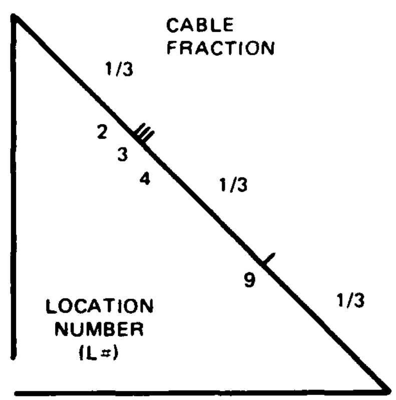

GUY CABLE

L#	CAPACITANCE ACTUAL	CAPACITANCE NEC	NEC Z_{21}	NEC ϕ
2	50.4	50.0	325.3	90.02
3	50.1	50.0	319.6	90.02
4	50.1	50.0	317.2	90.02
9	50.1	50.0	264.5	90.05

MEASURED

R_S = 1K	
Z_A	D
1043.0	-5.09

MEASURED

L#	R_S = 1K Z_{21}	R_S = 1K D	R_S = 5.1K Z_{21}	R_S = 5.1K D	R_S = 10K Z_{21}	R_S = 10K D
2	346.7	6.58	356.5	9.59	357.6	9.93
3	321.4	0.56	328.2	2.69		
4	309.5	-2.43				
9	242.8	-8.20				

UNITS: Z_A, OHMS
Z_{21}, OHMS
ϕ, DEGREES
D, PERCENT DIFFERENCE RE NEC
R_S, OHMS
CAPACITANCE, PICOFARADS, WITH FIXTURE

Figure A-11. Configuration 6, 50-pF set, Z_{21} and Z_A data.

FEEDPOINT

NEC	
Z_A	ϕ
1308.9	-89.96

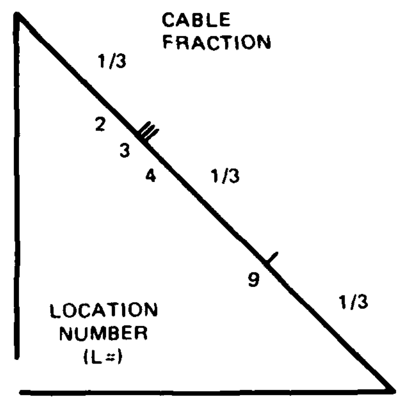

GUY CABLE

	CAPACITANCE		NEC	
L#	ACTUAL	NEC	Z_{21}	ϕ
2	11.7	11.0	417.0	90.02
3	11.7	11.0	387.8	90.02
4	11.6	11.0	377.5	90.02
9	11.6	11.0	224.4	90.09

MEASURED

$R_S = 1K$	
Z_A	D
1276.0	-2.51

MEASURED

	$R_S = 1K$		$R_S = 5.1K$	
L#	Z_{21}	D	Z_{21}	D
2	489.3	17.34	506.2	21.39
3			365.3	-5.80
4			331.2	-12.26
9			213.7	-4.77

UNITS Z_A, OHMS
Z_{21}, OHMS
ϕ, DEGREES
D, PERCENT DIFFERENCE RE NEC
R_S, OHMS
CAPACITANCE, PICOFARADS, WITH FIXTURE

Figure A-12. Configuration 6, 10-pF set, Z_{21} and Z_A data.

FEEDPOINT

NEC

Z_A	ϕ
961.7	-89.96

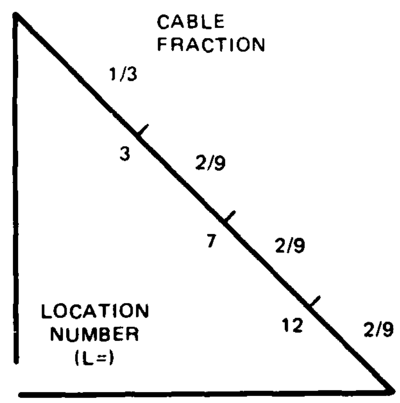

GUY CABLE

	CAPACITANCE		NEC	
L=	ACTUAL	NEC	Z_{21}	ϕ
3	50.4	50.0	473.8	90.02
7	49.4	50.0	344.8	90.03
12	50.1	50.0	288.0	90.05

MEASURED

R_S = 5.1K

Z_A	D
943.3	-1.91

MEASURED

R_S = 5.1K

L#	Z_{21}	D
3	477.7	0.82
7	344.8	0.0
12	275.4	-4.38

UNITS: Z_A, OHMS
Z_{21}, OHMS
ϕ, DEGREES
D, PERCENT DIFFERENCE RE NEC
R_S, OHMS
CAPACITANCE, PICOFARADS, WITH FIXTURE

Figure A-13. Configuration 7, 50-pF set, Z_{21} and Z_A data.

FEEDPOINT

NEC	
Z_A	ϕ
1232.5	-89.96

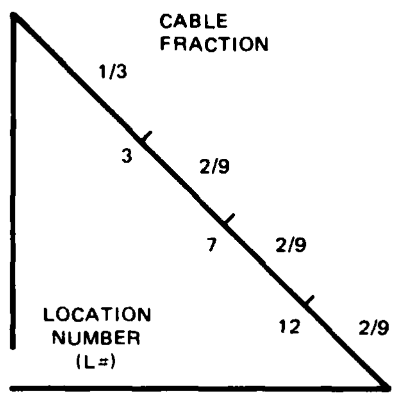

GUY CABLE

L#	CAPACITANCE ACTUAL	CAPACITANCE NEC	NEC Z_{21}	NEC ϕ
3	11.6	11.0	799.3	90.01
7	11.7	11.0	344.4	90.05
12	11.6	11.0	196.4	90.11

MEASURED

R_S = 5.1K

Z_A	D.
1189.0	-3.53

MEASURED

R_S = 5.1K

L#	Z_{21}	D
3	773.9	-3.18
7	312.2	-9.35
12	173.2	-11.81

UNITS: Z_A, OHMS
Z_{21}, OHMS
ϕ, DEGREES
D, PERCENT DIFFERENCE *RE* NEC
R_S, OHMS
CAPACITANCE, PICOFARADS, WITH FIXTURE

Figure A-14. Configuration 7, 10-pF set, Z_{21} and Z_A data.

FEEDPOINT

NEC	
Z_A	ϕ
1018.3	-89.96

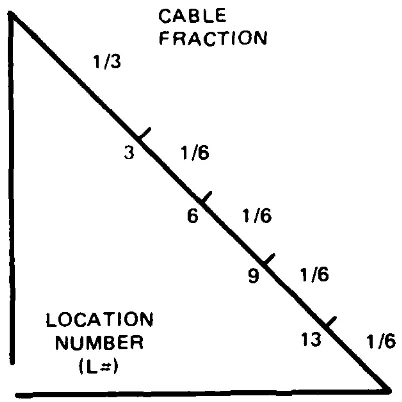

MEASURED

$R_S = 5.1K$

Z_A	D
991.4	-2.61

GUY CABLE

	CAPACITANCE		NEC	
L#	ACTUAL	NEC	Z_{21}	ϕ
3	50.4	50.0	415.5	90.01
6	50.1	50.0	300.3	90.03
9	49.4	50.0	233.1	90.05
13	50.1	50.0	202.7	90.06

MEASURED

$R_S = 5.1K$

L#	Z_{21}	D
3	425.9	2.50
6	299.0	-0.43
9	229.7	-1.46
13	192.1	-5.23

UNITS: Z_A, OHMS
Z_{21}, OHMS
ϕ, DEGREES
D, PERCENT DIFFERENCE RE NEC
R_S, OHMS
CAPACITANCE, PICOFARADS, WITH FIXTURE

Figure A-15. Configuration 8, 50-pF set, Z_{21} and Z_A data.

FEEDPOINT

NEC

Z_A	ϕ
1247.3	-89.96

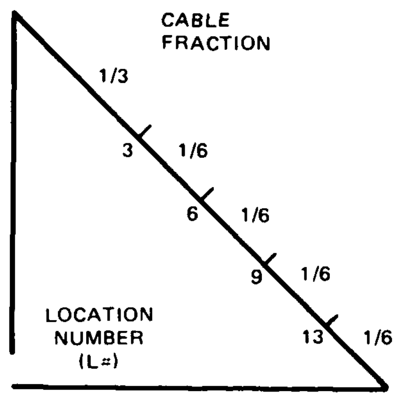

GUY CABLE

L#	CAPACITANCE ACTUAL	CAPACITANCE NEC	NEC Z_{21}	NEC ϕ
3	11.6	11.0	733.9	90.01
6	11.6	11.0	334.6	90.03
9	11.6	11.0	170.7	90.08
13	11.7	11.0	111.7	90.15

MEASURED

$R_S = 5.1K$

Z_A	D
1214.0	-2.67

MEASURED

$R_S = 5.1K$

L#	Z_{21}	D
3	715.3	-2.53
6	307.3	-8.16
9	148.8	-12.83
13	95.8	-14.23

UNITS: Z_A, OHMS
Z_{21}, OHMS
ϕ, DEGREES
D, PERCENT DIFFERENCE RE NEC
R_S, OHMS
CAPACITANCE, PICOFARADS, WITH FIXTURE

Figure A-16. Configuration 8, 10-pF set, Z_{21} and Z_A data.

FEEDPOINT

NEC	
Z_A	ϕ
1055.0	-89.96

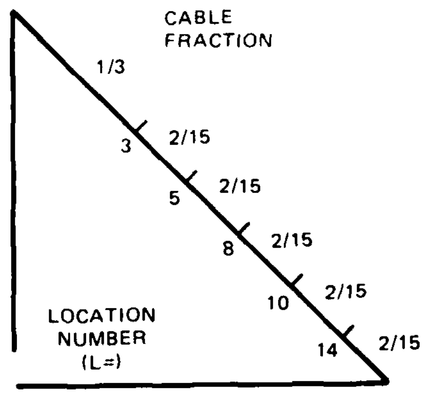

MEASURED
$R_S = 5.1K$

Z_A	D
1027.0	-2.65

GUY CABLE

	CAPACITANCE		NEC	
L#	ACTUAL	NEC	Z_{21}	ϕ
3	50.4	50.0	377.5	90.01
5	49.4	50.0	275.4	90.02
8	50.1	50.0	209.2	90.04
10	50.1	50.0	170.3	90.06
14	50.1	50.0	151.9	90.07

MEASURED
$R_S = 5.1K$

L#	Z_{21}	D
3	390.3	3.39
5	284.4	3.37
8	203.8	-2.58
10	161.3	-5.28
14	142.7	-6.06

UNITS: Z_A, OHMS
Z_{21}, OHMS
ϕ, DEGREES
D, PERCENT DIFFERENCE RE NEC
R_S, OHMS
CAPACITANCE, PICOFARADS, WITH FIXTURE

Figure A-17. Configuration 9, 50-pF set, Z_{21} and Z_A data.

FEEDPOINT

NEC	
Z_A	ϕ
1257.6	-89.96

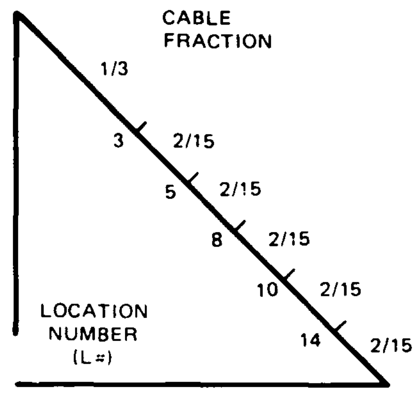

GUY CABLE

	CAPACITANCE		NEC	
L#	ACTUAL	NEC	Z_{21}	ϕ
3	11.7	11.0	686.4	90.00
5	11.7	11.0	331.6	90.02
8	11.6	11.0	171.2	90.06
10	11.6	11.0	99.7	90.12
14	11.6	11.0	71.7	90.19

MEASURED

R_S = 5 1K

Z_A	D
1214.0	-3.47

MEASURED

R_S = 5.1K

L#	Z_{21}	D
3	671.9	-2.11
5	308.7	-6.91
8	152.9	-10.69
10	84.8	-14.94
14	60.9	-15.06

UNITS Z_A, OHMS
Z_{21}, OHMS
ϕ, DEGREES
D, PERCENT DIFFERENCE RE NEC
R_S, OHMS
CAPACITANCE, PICOFARADS, WITH FIXTURE

Figure A-18. Configuration 9, 10-pF set, Z_{21} and Z_A data.

APPENDIX B

PARAMETERS CALCULATED WITH THE NEC

C# and L# refer, respectively, to the numbers assigned to each test configuration and fixture location. Each is defined in Figure 2 and Appendix A.

The input currents at the feedpoint and the output voltages on the capacitors are the result of a 1-volt rms driving potential. For some test configurations, the sum of capacitor voltages exceeds 1 volt, as was expected. The magnitudes of the mutual impedances, Z_{21}, and feedpoint impedances, Z_A, equal the ratios of input voltage and current and of output voltage and input current, respectively. The radiation resistance, R_r, was also calculated and included.

The phase of the input signal is essentially 90 degrees, indicating a leading current and a capacitive input characteristic. This is also reflected in the negative phase angles shown with Z_A.

While the test set that used the nominally 10-pF capacitors is referred to as the 10-pF set, the calculations were based on 11 pF in order to include the effects of holding fixture capacitances.

Table B-1. NEC results for the 10-pF set; see page B-1 for definitions.

		Current Input		Voltage Output		Z_{21}		Z_A		R_r
C#	L#	$A \times 10^{-3}$	Deg	V	Deg	Ohms	Deg	Ohms	Deg	Ohms
1	6	1.0135	89.96	1.1436	179.995	1128.367	90.035	986.69	-89.96	0.5986
2	1	0.8380	89.87	1.1192	179.998	1335.540	90.028	1193.30	-89.97	0.5031
3	11	1.2280	89.96	1.2162	179.993	990.391	90.033	814.33	-89.96	0.5601
4	3	0.8284	89.96	0.7516	179.979	907.291	90.079	1207.00	-89.96	0.7487
	9			0.3381	180.034	408.124	90.074			
5	3	0.7849	89.96	0.4376	179.979	557.474	90.019	1274.10	-89.96	0.7857
	4			0.4213	179.980	536.795	90.020			
	9			0.2208	180.062	281.368	90.102			
6	2	0.7640	89.96	0.3186	179.978	417.036	90.018	1308.90	-89.96	0.8018
	3			0.2963	179.980	387.769	90.020			
	4			0.2884	179.980	377.468	90.020			
	9			0.1715	180.085	224.447	90.090			
7	3	0.8113	89.96	0.6485	179.970	799.294	90.010	1232.50	-89.96	0.7985
	7			0.2794	180.008	344.381	90.048			
	12			0.1594	180.072	196.416	90.112			
8	3	0.8018	89.96	0.5884	179.969	733.869	90.009	1247.30	-89.96	0.8206
	6			0.2682	179.993	334.568	90.033			
	9			0.1368	180.041	170.664	90.081			
	13			0.0896	180.110	111.743	90.150			
9	3	0.7952	89.96	0.5458	179.960	686.431	90.000	1257.60	-89.96	0.8327
	5			0.2637	179.980	331.589	90.020			
	8			0.1361	180.020	171.183	90.060			
	10			0.0793	180.077	99.664	90.117			
	14			0.0570	180.149	71.707	90.189			

Table B-2. NEC results for the 50-pF set; see page B-1 for definitions.

		Current Input		Voltage Output		Z_{21}		Z_A		R_r
C=	L=	A × 10^{-3}	Deg	V	Deg	Ohms	Deg	Ohms	Deg	Ohms
1	6	1.78	89.976	1.3592	179.994	763.596	90.018	561.80	-89.98	0.2414
2	1	1.55	89.984	1.329	179.996	857.419	90.012	641.80	-89.98	0.1731
3	11	2.0761	89.970	1.46	179.992	703.275	90.022	481.66	-89.97	0.2505
4	3	1.15	89.971	0.6661	179.988	579.191	90.017	869.57	-89.97	0.4421
	9			0.5149	180.005	447.774	90.034			
5	3	0.9908	89.960	0.4077	179.980	411.480	90.020	1009.30	-89.96	0.5391
	4			0.4037	179.990	407.450	90.030			
	9			0.3251	180.010	328.120	90.050			
6	2	0.91	89.969	0.2961	179.988	325.341	90.019	1098.90	-89.97	0.5973
	3			0.2908	179.989	319.571	90.020			
	4			0.2887	179.990	317.220	90.021			
	9			0.2407	180.023	264.451	90.054			
7	3	1.0399	89.960	0.4927	179.980	473.766	90.020	961.65	-89.96	0.5606
	7			0.3586	179.990	344.802	90.030			
	12			0.2995	180.010	288.008	90.050			
8	3	0.9820	89.960	0.4080	179.970	415.513	90.010	1018.30	-89.96	0.6309
	6			0.2949	179.990	300.257	90.030			
	9			0.2289	180.010	233.129	90.050			
	13			0.1991	180.020	202.711	90.060			
9	3	0.9479	89.960	0.3578	179.970	377.506	90.010	1055.00	-89.96	0.6756
	5			0.2611	179.980	275.425	90.020			
	8			0.1983	180.000	209.183	90.040			
	10			0.1614	180.020	170.254	90.060			
	14			0.1440	180.030	151.929	90.070			

END
DTIC
8-86